Investigation of the surface structure of colloidal platinum by infrared spectroscopy of adsorbed CO†

Dominique de Caro and John S. Bradley*

Max-Planck-Institut für Kohlenforschung, Kaiser-Wilhelm-Platz 1, D-45470 Mülheim an der Ruhr, Germany

The infrared spectra of ^{12}CO and of ^{12}CO–^{13}CO mixtures adsorbed on poly(vinylpyrrolidone)-stabilized colloidal platinum in liquid dispersion are reported. Comparison with the vibrational spectra reported for analogous supported Pt particles shows the absence of detectable terrace sites on the colloidal particles. Spectral features resulting from vibrational coupling between the adsorbed CO molecules are analysed in terms of the structure and sizes of the metal particles and the adsorption sites available for CO.

Highly dispersed transition metals in the colloidal state are interesting liquid phase analogues to supported metal catalysts, and an understanding of the nature of the surfaces of these metal particles is important in the context of their liquid phase catalytic application. It is preferable that the surfaces of colloidal metal catalysts be investigated in the liquid phase, that is to say in the same environment in which their catalytic properties are evaluated. Accordingly, we[1–10] and others[11–16] have investigated the surface composition and structure of colloidal metals and alloys in liquid dispersion by spectroscopic investigations of adsorbates, predominantly CO, on colloidal metals, with a view to adding to our understanding of this aspect of colloidal metal surface chemistry.

The high infrared extinction coefficient of adsorbed CO has made this chromophore the most widely investigated adsorbate in surface science, and the structural surface chemistry of CO on elemental metal and alloy crystal surfaces is well-developed. Detailed spectroscopic data accumulated for adsorbed CO on single crystal faces have been relied upon in the characterization of the surface chemistry of CO on small metal particles, and have allowed the use of vibrational spectroscopy as a probe of the surface compositions and structures of highly dispersed supported metal catalysts.

Metal particles in colloidal liquid dispersion are particularly ammenable to this approach, since even at high particle concentrations the dispersions do not appreciably scatter infrared radiation, and so relatively high extinction infrared absorptions can be obtained in transmission mode. Another advantage for the study of CO on colloidal metals is that the absorption equilibrium is reached rapidly during addition of the gaseous adsorbate to the liquid dispersion, due to the absence of the diffusion barriers that may exist in solid samples. For example, on exposure of colloidal metal samples to CO we routinely observe saturation spectra after only a few minutes, compared to CO adsorption equilibration times of 200 h reported for Pt–SiO_2 in the form of a pressed wafer.[17]

The application of infrared spectroscopy to the analysis of colloidal metal surfaces has been developed in several laboratories, and the spectra of CO adsorbed on hydrosols of platinum, palladium[12–15] and rhodium,[16] and on organosols of nickel,[9] palladium,[1,3–5] platinum,[2,5,10,11,18] ruthenium[5] and palladium–copper alloys[6–8] have been reported. Initially the analysis of spectra was limited to the assignment of frequencies for the various bonding geometries for CO—triply and doubly bridging and terminal ('on top') modes. The relative extinctions for the absorption bands associated with the various adsorbed states of CO were correlated with particle size in the case of colloidal palladium,[3,4] by analogy to similar correlations on supported metal particles.[19,20] In general, the results for colloidal metals are similar to those for supported metal particles. For example, polymer-stabilized colloidal palladium adsorbs CO predominantly on bridging sites, with a low abundance of linear CO at higher coverages, whereas the analogous colloidal platinum adsorbs CO predominantly on linear sites, with a low occupancy of bridged sites. This is also the general observation for supported platinum and palladium particles.[21] While this in no way makes a case for the improbable idea that the colloidal metal particles are 'clean' in the as-prepared state, it does suggest that CO can adsorb on the colloidal metal surfaces in a manner that can be interpreted by reference to the corresponding 'clean' system. We therefore consider it useful to pursue the analysis of the surfaces of colloidal metal particles by experiments that parallel those on single crystal and supported metal systems.

We have recently conducted further IR spectroscopic studies of CO adsorbed on colloidal nickel and platinum,[9,10] and we report here in detail an FTIR study of ^{12}CO and ^{12}CO–^{13}CO mixtures adsorbed on colloidal platinum stabilized with poly(vinylpyrrolidone) (PVP). In these experiments we focus on both the infrared absorption frequencies of adsorbed CO and on additional phenomena, which arise from vibrational interactions between the CO molecules in the adsorbed overlayer and which are characteristic of CO adsorbed on single crystal metal surfaces and supported metal crystallites. These phenomena manifest themselves as coverage dependent frequency shifts and as non-linear intensity ratios for ^{12}CO–^{13}CO mixtures. Since the underlying interactions between the adsorbate molecules that give rise to these effects are dependent on the presence and extent of domains of adsorbed CO, their observation can provide information on the structure of the metal surface, which is difficult to obtain for colloidal metal dispersions. Thus, if a colloidal metal preparation contains particles with highly irregular surfaces with many defect sites, the abundance of domains of CO would be diminished and vibrational coupling would be impaired. Similarly, the presence of the stabilizing polymers used to protect the colloidal particles in liquid dispersion might also interfere with the assembly of the adlayer of CO on the metal surface.

The colloidal platinum samples we will analyse in this study are prepared from the reaction of a zerovalent organometallic complex of the metal, $Pt_2(dba)_3$[5,22] (dba = dibenzylideneacetone), with hydrogen or with carbon monoxide. These preparations result in metal particles in the size range of 1–2

* E-mail: bradley@mpi-muelheim.mpg.de
† Non-SI unit employed: 1 bar = 10^5 Pa.

nm; at these particle sizes it is often not clear from electron microscopy whether or not the particles are well-formed with facetted surfaces and additional techniques, such as those we describe here, must be applied in order to describe the nature of the particle surface.

An IR flow cell coupled to a remote detector was designed with the goal of allowing continuous measurement of the IR spectra of adsorbed CO at a range of coverages, and of the exchange reaction of ^{12}CO and ^{13}CO on the colloidal metal surfaces.

Experimental

The colloids which we have analysed might be expected to exhibit some degree of air sensitivity and so we have adopted the general precautions that are common practice in the synthesis of moderately air sensitive compounds such as molecular carbonyl clusters. All manipulations were carried out using standard Schlenk tube or Fischer–Porter bottle techniques under an Ar atmosphere. Poly(vinylpyrrolidone) (MW 40000; Aldrich) was previously dried under dynamic vacuum at 90 °C for 3 h. Dichloromethane was distilled under an atmosphere of argon from calcium hydride. $Pt_2(dba)_3$[23] was prepared according to literature procedures.

Preparation of the colloids

Reaction of $Pt_2(dba)_3$ with carbon monoxide: 1.0 nm Pt–PVP. $Pt_2(dba)_3$ (16 mg, 0.029 mg atom Pt, 5.6 mg Pt) and PVP (184 mg, Pt/PVP = 3 wt%) were dissolved in 20 mL of dichloromethane. A slow stream of CO, saturated with dichloromethane, was passed through the solution for 5 min during which time the colour of the solution turned from purple to yellow-brown. The solvent was then removed under reduced pressure and the solid stored under argon. The resulting material contained platinum particles with an approximate mean diameter of 1.0 nm, as shown by TEM (transmission electron microscopy).

Reaction of $Pt_2(dba)_3$ with hydrogen: 1.5 nm Pt–PVP. $Pt_2(dba)_3$ (16 mg, 0.029 mg atom Pt, 5.6 mg Pt) and 184 mg of PVP (Pt/PVP = 3 wt%) were dissolved in 20 mL of dichloromethane in a Fisher–Porter bottle. The resulting purple solution was then stirred vigorously under hydrogen (2 bar). After 1 day the colour of the solution had turned from purple to brown. After 2 days the solvent was evaporated under reduced pressure and the solid stored under argon. The resulting material contained platinum particles with a mean diameter of 1.5 nm, as shown by TEM.

Remote detection infrared flow system

A schematic of the infrared detection flow system is shown in Fig. 1. The infrared beam for the remote experiment passes *via* the beam splitter of a Nicolet Magna 550 FTIR spectrometer to an external optical bench (Axion Analytical), coupled to the Passport™ external optics port of the spectrometer. The IR beam passes through a flow cell (CaF_2 windows, pathlength variable from 0.05–2 mm) to a remote MCT detector (Graseby). Spectra were obtained at 8 cm^{-1} resolution and accumulated at 10 s^{-1}. The colloidal metal suspensions were made up using *ca.* 200 mg of solid Pt–PVP in 20 mL of dry dichloromethane under argon in a 100 mL Schlenck tube. A volume of 20 mL proved sufficient to fill the transfer lines, pump and transmission IR cell, with *ca.* 5 mL as a gas absorption reservoir remaining in the Schlenck tube. The colloidal suspension, which at these concentrations was a mobile non-viscous liquid, was passed through the IR cell *via* 2 mm polyethylene tubing using a circulating pump (Cole–Palmer model 7144–05) at a rate of 300 mL min^{-1}. The inlet and outlet of

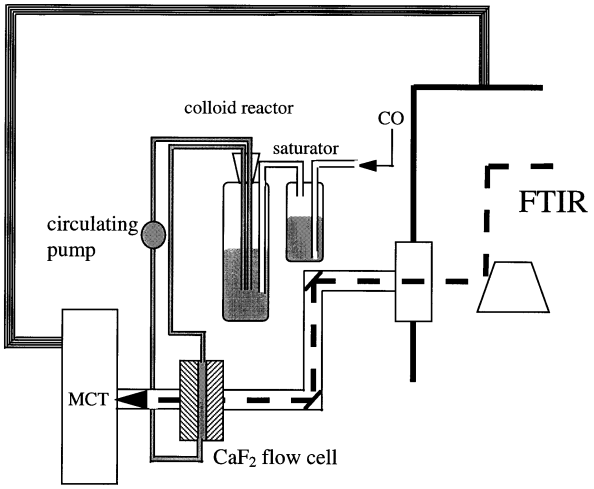

Fig. 1 Schematic drawing of the FTIR flow experiment. For a description see text

the circulation line were kept under the surface of the colloid suspension to minimize bubble formation. Since the FTIR experiment involved accumulation of many spectra, spectral artifacts caused by occasional bubbles passing through the cell were averaged out. The reservoir was not stirred, agitation being accomplished only by the constant influx of liquid from the return line. This allowed for a slow saturation of the solution with CO, which contributed to the good temporal resolution of the experiment. Addition of CO in a slow stream (*i.e.*, one bubble per second) to the colloid suspension was made *via* a saturator containing dichloromethane, so that during the course of the experiment the concentration of the colloid remained constant. This allowed the precise subtraction of the relatively intense solvent and polymer overtone and combination bands in the 2200–1800 cm^{-1} region of the initial spectrum from all subsequent spectra during CO addition. The resulting spectra thus contained only absorptions due to adsorbed CO on the colloidal metal particles and dissolved CO.

In a typical experiment the colloid suspension, under argon, was circulated through the IR cell for one minute and then data acquisition begun. After collecting the initial spectrum, to be subtracted from all subsequent spectra, addition of CO was begun and data collection continued for up to 1 h. After this time the spectra were batched and averaged for time intervals of 1.17 s, the starting spectrum subtracted, and the resulting spectra of adsorbed CO displayed in a manner that depended on the rate of change of the spectrum. Saturation was achieved in all cases after several minutes. For $^{12}CO/^{13}CO$ exchange experiments the process was begun by initial addition of ^{13}CO, until saturation of the colloidal metal surface was acheived, as measured by a constant intensity in all the IR bands associated with^{13}CO, and then the gas stream was switched to ^{12}CO. The experiment was then continued with slow passage of ^{12}CO until complete replacement of ^{13}CO with ^{12}CO was achieved, which in all cases was in less than one hour.

Results

The colloid prepared from $Pt_2(dba)_2$ by treatment with hydrogen or CO in dichloromethane in the presence of PVP, and shown by TEM to contain particles with mean diameters of 1.5 nm (Pt–H_2) and approximately 1.0 nm (Pt–CO), are designated as **Pt-15** and **Pt-10**, respectively.

IR spectra at partial and full coverage of ^{12}CO

The direct measurement of partial ^{12}CO coverage spectra was possible only for the **Pt-15** sample since **Pt-10** was prepared

under, and therefore saturated with, CO. Although thermal desorption of CO could provide partial coverage spectra for this colloid, the disruption of the adsorbed CO overlayer on platinum nanoclusters is reported to lead to significant restructuring of the particles.[22]

Spectra of **Pt-15** recorded during slow addition of ^{12}CO are shown in Fig. 2. At maximum coverage the spectrum shows a strong absorption at 2045 cm^{-1} plus a weak band at 1875 cm^{-1}. There is also a weak band at 2090 cm^{-1}, which is not always present in the spectra of similar $Pt–H_2$ preparations, and which we assign to CO on oxidized sites occasionally present in low abundance on the particles. Intentional exposure of the colloidal sample to air for 1 h resulted in an increase in intensity of this band. Both the 2045 and 1875 cm^{-1} bands show a significant shift to lower frequencies at lower CO coverage. A coverage dependent shift of 25 cm^{-1} in the higher frequency band is observed on going from the lowest coverage in the first spectrum, measured after 5 s of CO addition, to the maximum coverage, reached after approximately 48 s. Spectra recorded during a further 15 min of CO addition showed no increase in intensity of the band at 2045 cm^{-1}, and no change in frequency. However, after the adsorbed CO band has reached its maximum intensity a new band at 2137 cm^{-1} appears, due to free dissolved CO, and grows to a maximum intensity between 1 and 15 min.

The full coverage spectrum for ^{12}CO on **Pt-15** is shown in Fig. 3, and in Fig. 4 is shown the spectrum obtained for **Pt-10** at full coverage of ^{12}CO, obtained after complete exchange of ^{13}CO by ^{12}CO, as described in the following section.

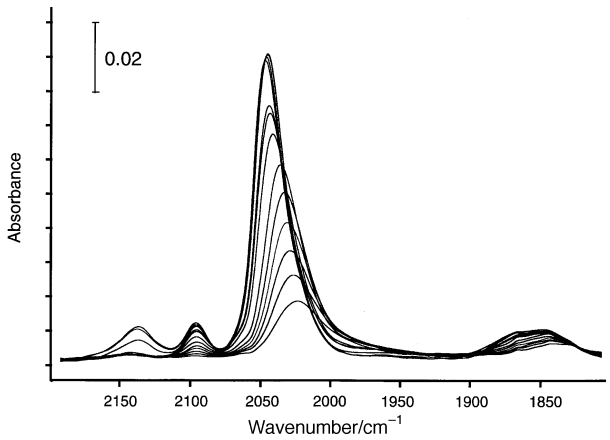

Fig. 2 FTIR spectra during addition of CO to 1.5 nm Pt–PVP (**Pt-15**) for 15 min. The first spectrum corresponds to 5 s from the start of CO addition, and maximum intensity is reached after 48 s

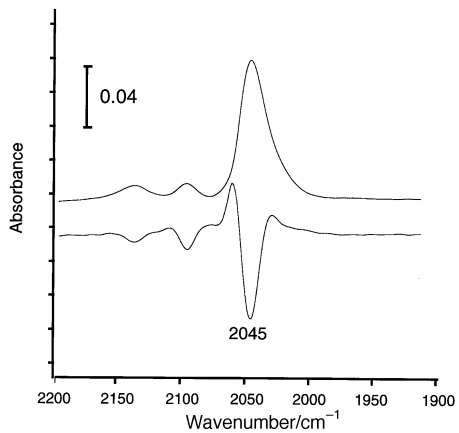

Fig. 3 FTIR spectrum of CO at maximum coverage on **Pt-15** (extracted from Fig. 2) showing the second derivative

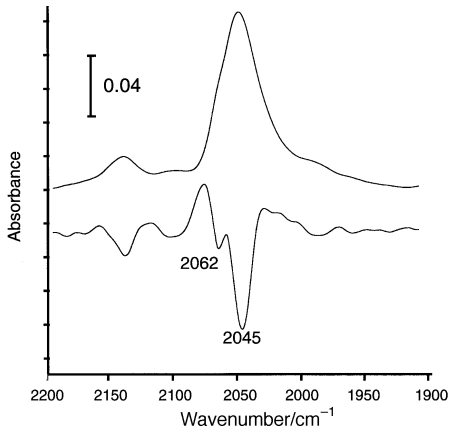

Fig. 4 FTIR spectrum of CO at maximum coverage on **Pt-10** [extracted from Fig. 5(*a*)] showing the second derivative

IR spectra during $^{13}CO/^{12}CO$ exchange

In the $^{13}CO/^{12}CO$ exchange experiment with **Pt-10,** the starting dispersion was prepared by treatment of $Pt_2(dba)_3$ with ^{13}CO, and with **Pt-15** by prior formation of the colloid from $Pt_2(dba)_3$ under hydrogen, and subsequent saturation with ^{13}CO.

Infrared spectra obtained during replacement of ^{13}CO, initially at maximum coverage, by ^{12}CO, are shown in Figs. 5(*a*) (**Pt-10**) and 5(*b*) (**Pt-15**). The corresponding superimposed spectra for each sample are shown in Figs. 6(*a*) and 6(*b*).

For **Pt-10** and **Pt-15** the spectra corresponding to adsorption of 100% ^{13}CO show bands at 1999 and 1998 cm^{-1}, respectively, with much lower intensity bands below 1900

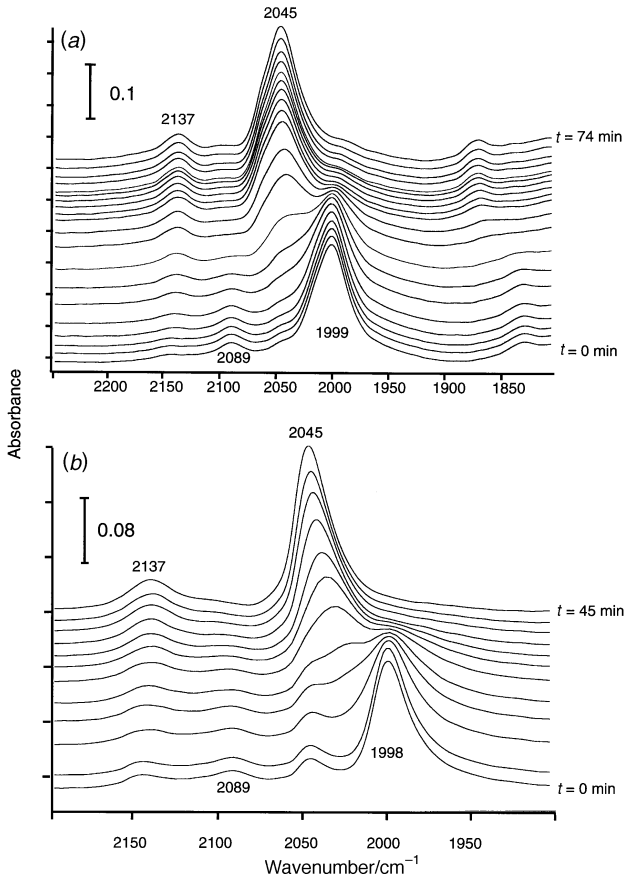

Fig. 5 FTIR spectra obtained during exchange of ^{13}CO adsorbed on (*a*) 1.0 nm Pt–PVP (**Pt-10**) or (*b*) 1.5 nm Pt–PVP (**Pt-15**) by ^{12}CO

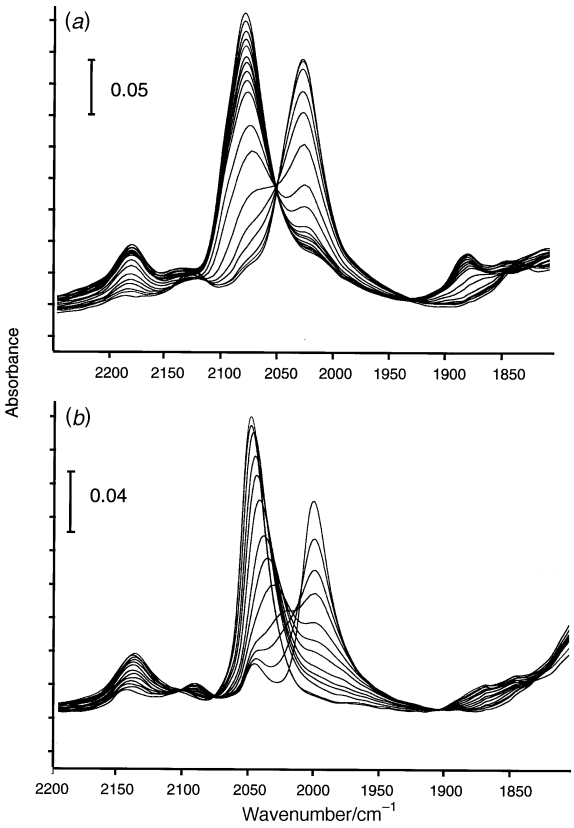

Fig. 6 Overlayed spectra from (*a*) Fig. 5(*a*) and (*b*) Fig. 5(*b*)

cm^{-1}. Spectra obtained during the addition of ^{12}CO to the ^{13}CO-covered platinum colloids show a steady replacement of ^{13}CO by ^{12}CO over a period of approximately 60 min. The reaction is also matched by the replacement of a low intensity band at 2090 cm^{-1}, due to dissolved ^{13}CO, with a band of similar intensity at 2137 cm^{-1}, due to ^{12}CO. Spectra obtained during the exchange process, corresponding to intermediate isotopic compositions but at constant total coverage, show steadily decreasing intensity in the low frequency components of the spectra with concurrent increase in intensity in the high frequency component. After complete exchange with ^{12}CO, the bands at 1999 and 1998 cm^{-1} for **Pt-10** and **Pt-15** are replaced by an absorption at 2045 cm^{-1}.

The overlayed absorbance spectra recorded during the $^{13}CO/^{12}CO$ exchange reaction exhibit an isosbestic point at 2020 cm^{-1} for the **Pt-10** colloid [Fig. 6(*a*)] whereas the corresponding spectra for the **Pt-15** sample show no such isosbestic point [Fig. 6(*b*)].

Discussion

In the following discussion we rely, in our interpretation of the spectra obtained with colloidal metals, on published data for the better understood supported metal and single crystal systems. However, it must be stressed at the outset that these experiments are not designed to demonstrate a preconceived similarity between the surfaces of crystalline or supported metals on the one hand, and colloidal metal particles in liquids on the other. Rather they intend to use a method established for the surface analysis of metals, in both single crystal or supported form, to shed light on the surfaces of small metal particles in the colloidal state. In fact, as will be seen, we reach the conclusion that the surfaces of these small metal particles, prepared under mild conditions, are significantly different from those of supported metal particles of similar size, due to the fact that the latter are prepared under conditions that allow annealing of the surfaces to stable crystal faces.

The discussion will be divided into three parts, describing full coverage ^{12}CO spectra, partial coverage spectra, and $^{13}CO/^{12}CO$ exchange spectra.

Full coverage ^{12}CO spectra

As shown in Figs. 3 and 4, the spectra at maximum coverage on both **Pt-15** (after direct saturation with ^{12}CO) and **Pt-10** (after exchange of ^{13}CO with ^{12}CO), which are dominated by a band at 2045 cm^{-1}, are assigned as usual to CO bound to single platinum atoms. The much lower intensity and broader band between 1850 and 1950 cm^{-1} is assigned to CO in two-fold bridging sites. We will limit dicussion of the spectra to the dominant >2000 cm^{-1} band.

The spectra can be compared with those obtained for CO adsorbed on supported Pt–SiO_2 samples in a range of sizes from 1.1–10 nm, which show three bands of varying intensity in the frequency ranges near 2080, 2070 and 2060 cm^{-1}.[17,24] These bands were assigned to CO adsorbed on face, edge and vertex sites on the particles, based on a comparison with single crystal data obtained for CO on a Pt(111) surface, which ideally contains only nine-coordinate platinum atoms in terrace sites, a Pt(533) surface, containing terraces with seven-coordinate platinum atoms at (100) steps, and a Pt(432) surface, containing terraces with six-coordinate platinum atoms at kinked steps. The highest frequency of the three bands, usually at >2080 cm^{-1}, was assigned to CO on terrace sites. The Pt(111) faces, which since they contain metal atoms in the maximum surface coordination number of 9 are thermodynamically the most stable, might be expected to be found for most Pt particles. However, for the colloidal samples, in the maximum coverage ^{12}CO spectra for **Pt-10** (Fig. 4) and **Pt-15** (Fig. 3), no bands of similar frequency to CO in terrace sites on Pt–SiO_2 are observed.

It is unlikely that the surface electronic environment of the colloidal metal particles is so intrinsically different from that of supported metal particles of similar size that the 2045 cm^{-1} band could correspond to a terrace-bound CO. A shift might be expected due to the fact that spectra for the colloidal samples were obtained in liquid dispersions. Medium effects are known to be significant in reducing the vibrational frequencies of molecular metal carbonyl complexes in going from the vapour to the solution state, but this could account for a shift of only *ca.* 10 cm^{-1}.[25] A more problematic issue is that of the possible consequences of co-adsorption of the stabilizing polymer and byproducts from the colloid preparation, which cannot be ruled out, and these potential effects are difficult to quantify. The presence of polymer and/or byproducts might be expected to break up islands of CO, mitigate vibrational coupling, and result in a lower full coverage frequency than would otherwise be expected. However, this argument would only apply to the smaller **Pt-10** particles, since vibrational coupling is in fact observed for the **Pt-15** particles (see below for a discussion of vibrational coupling effects.) However, even allowing for shifts induced by solvent and adventitious co-adsorbates, it is difficult to conclude, in the absence of any bands >2050 cm^{-1}, that any two-dimensional arrays of CO on terrace sites are present on the surfaces of these colloidal platinum clusters.

For a preparation containing much larger colloidal platinum particles (a 3.5 nm Pt–PVP colloid prepared by reduction of $PtCl_6^{2-}$ in aqueous methanol[26,27]), the highest frequency absorption we observe at maximum coverage of ^{12}CO is at 2065 cm^{-1},[28] and based on the present assignments even these larger particles, which we have previously shown to be monocrystalline,[27] present no detectable terraces for CO adsorption. This seems surprising in view of the regular structure of the particles, but a recent high resolution

TEM study on even larger platinum particles[29] supports this conclusion. In that work, exceptionally geometrically regular, monocrystalline platinum particles[30,31] were imaged, and despite the fact that the bulk structures of the particles are devoid of defects or twin planes, images of the surfaces reveal a high incidence of defects in the form of one- or two-atom steps and kinks. The surfaces of metal particles prepared under the mild conditions used in colloidal metal preparations have not been exposed to conditions that would cause annealing to the most stable surface structure, and in this they differ from supported platinum particles in heterogeneous catalysts, which are usually subjected to thermal annealing before use. We thus conclude that, because of the mild conditions used for the preparation of colloidal metals, *highly defected surfaces are the rule, and not the exception.*

The two bands at lower frequencies reported by Brandt *et al.*[17] for ^{12}CO on Pt–SiO_2, at *ca.* 2070 and 2060 cm^{-1}, were assigned to CO adsorbed on vertex and edge sites of the platinum particles, respectively, and these are of relevance to the colloidal system. The assignment of the lower frequency band to the higher coordination number metal (edge) site was seen as surprising, but the spectra we observe are consistent with this assignment, if we allow a discrepancy of *ca.* 10 cm^{-1} shift due to medium effects. For the smallest particles, even if they were of regular geometry, it is expected that most surface atoms are vertex or edge (low coordination number) atoms. A re-examination of the surface statistics for regular polyhedral arrays of atoms, taking the example of a cuboctahedral fcc particle,[32] shows that only at the lowest particle sizes, when the polyhedral edge contains $\leqslant 3$ atoms, is a significant proportion of vertex atoms present. For larger particles with regular cuboctahedral edges of 3–6 atoms, edge atoms predominate, but terrace sites also grow in number. For example, for a cuboctahedron of 38 atoms (two atoms on each edge), which is the model used by Brandt *et al.* for a 1.1 nm Pt particle,[17] 24 of the 32 surface atoms, 75%, are vertex atoms, and 25% are terrace atoms. For the next largest regular cuboctahedron with three atoms on an edge and comprising 201 atoms, 30% of the 122 surface atoms are edge sites, the proportion of vertex atoms falls to 20%, but a further 45% are also (111) terrace sites, as shown in Fig. 7(*a*). Our assertion that essentially no terrace sites are available on the particles we report here, which fall in the size range in which a significant abundance of terrace sites would be expected for a regular cuboctahedral particle, requires the addition of only 24 capping atoms to the terraces of the regular cuboctahedron of this size, giving the 'max-B_5' structure,[32] shown in Fig. 7(*b*), in which case the proportion of terrace sites falls to zero, even for this regular morphology.

The preceding argument concerns close-packed regular geometries, but there is no reason to assume a closed regular geometry for any of the particles we discuss here. However, the general argument holds for less regular morphologies, which would have an even higher incidence of surface defect sites. In either case we propose that **Pt-10** approximates the first of the two cases described, with a preponderance of edge and vertex sites, and that **Pt-15** falls into the second category, with more edge sites than vertex sites, but no terrace sites. The spectra for CO on **Pt-10** and **Pt-15** can now be assigned on this basis by comparison with the assignments of Brandt *et al.*[17]

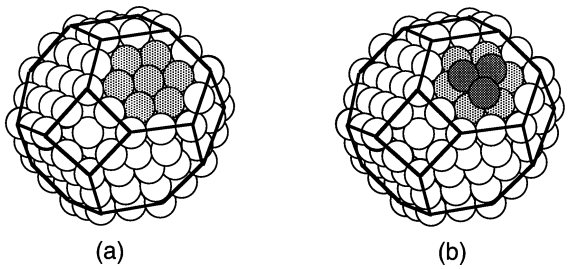

Fig. 7 (*a*) Regular cuboctahedron with three atoms on a side; (111) terrace atoms are shaded. (*b*) Same as (*a*) but with 24 adatoms added, three to each of the eight (111) terrace sites (max-B_5 structure)

In the full coverage ^{12}CO **Pt-10** spectrum, Fig. 4, extracted from the final spectrum in the $^{12}CO/^{13}CO$ exchange experiment, we would expect a convolution of two bands corresponding to vertex (higher frequency) and edge (lower frequency) sites. The presence of a high frequency shoulder at 2062 cm^{-1}, discernable on the principal 2045 cm^{-1} band, is confirmed by the minimum at this frequency in the second derivative trace superimposed on the absorbance spectrum. We assign this higher frequency band to vertex-bound CO, and the 2045 cm^{-1} band to edge-bound CO. The relative amounts of the two CO binding sites will depend on the detailed geometry of the particle. These observations are generally consistent with the IR absorption at 2050 cm^{-1} reported[22] for 1.3 nm platinum clusters prepared in the absence of a stabilizing polymer by a similar reaction to that used for the preparation of **Pt-10.**

The full coverage ^{12}CO spectrum for **Pt-15**, shown in Fig. 3, shows only a single band, with no trace of a secondary minimum in the second derivative trace. Thus the spectrum is dominated by vibrations due to edge-bound CO, but given the resolution of the experiment we cannot rule out the presence of vertex-bound CO if the corresponding absorption is close to that of the edge-bound CO.

Partial coverage and $^{12}CO/^{13}CO$ exchange spectra

In addition to the structural information derived from the full coverage ^{12}CO spectra discussed above, a second approach to providing structural insights for the colloidal clusters is possible from a series of vibrational spectra under conditions of partial coverage of ^{12}CO or full coverage of a constantly changing set of ^{12}CO–^{13}CO mixtures. The literature on vibrational spectroscopy of CO on metal surfaces describes the phenomena that can occur under such conditions[33,34] and which can reveal in some detail the structure of the adsorbed CO overlayer, and by extension the structure of the underlying metal surface. The phenomena will be briefly summarized to provide a basis for discussion of the colloid spectra.

Spectra often show a coverage dependent frequency shift in the CO vibrational bands, and this provides an important piece of evidence concerning the spatial distribution of the adsorbed CO molecules and the nature of the underlying metal surface. This effect was originally observed by Eischens and Pliskin for CO at partial coverage on supported Pt,[35] and by Crossley and King in a study of ^{13}CO–^{12}CO mixtures on Pt(111).[36] Extensive investigations of the vibrational spectra of CO on other single crystal surfaces and on small crystallites have been made,[17,24,37–40] and in these and many other studies coverage dependent frequency shifts have been observed for adsorbed CO. In pairs of absorptions associated with ^{13}CO–^{12}CO mixtures adsorbed on metal surfaces the high frequency band also exhibited a marked shift to higher frequency as the ^{13}CO is replaced by ^{12}CO, but the lower frequency band showed a much smaller shift with changing isotopic composition. These effects arise from vibrational interactions between the CO molecules in the adsorbed overlayer, which occur in the presence of domains of adsorbed CO.[35,36,41–43] The coupled CO oscillators act as an extended domain, the structure of which reflects a balance between site-specific interactions (maximizing M–CO interactions) and CO–CO repulsive interactions, favouring close packing of CO in the adsorbed overlayer at high coverages.

An additional consequence of vibrational coupling is observed in spectra for mixtures of ^{12}CO and ^{13}CO on metal surfaces. Not only do the frequencies of each isotopomer vary

in the manner expected with dilution (*i.e.*, decreasing frequency with decreasing coverage) but a transfer of intensity is observed from the lower frequency to the higher frequency absorption. Thus, over a range of isotopic compositions, mixtures of ^{12}CO and ^{13}CO will give rise to spectra in which the relative intensities of the principal bands will not reflect the relative abundance of the two isotopomers. In systems in which coupling is significant, single isotope spectra will also be distorted if two or more vibrationally distinguishable CO adsorption sites are present, since the high frequency band will acquire intensity at the expense of the low frequency component, thus distorting the combined spectrum. In such cases a greater apparent shift with increasing coverage than expected will be observed, and the original reports of shifts of up to 40 cm^{-1} have been shown to be due to the superimposition (with intensity transfer) of absorptions due to CO on different sites with different (but not necessarily resolvable) frequencies, each with its own coverage dependent shift.[42]

The range over which this coupling occurs extends over many surface atoms, and is greatest when the vibrating molecules are closest together. Hollins has concluded[42] that only at the smallest island sizes will the coupling differ significantly from that observed for an infinite surface. Moskovits and Hulse suggested that poorly ordered metal surfaces, with many defect sites, will prevent the assembly of more highly coupled, larger domains of CO and vibrational coupling would, under these circumstances, be mitigated.[41] On the basis of these correlations we will use the presence or absence of this phenomenon as an indicator of the surface structure of the colloidal metal particles that are the subject of the current investigation.

Partial coverage spectra. As shown in Fig. 2, the linear CO stretching band for CO on **Pt-15** is first observed at 2020 cm^{-1}, with an absorbance that is approximately 13% of that reached at saturation. This band shifts to 2045 cm^{-1} as maximum coverage is reached after *ca.* 1 min. During this time no measurable concentration of dissolved CO can be detected. Subsequently, the free CO concentration increases to a saturation value as shown by the growth of a band at 2137 cm^{-1} with no further increase in the adsorbed CO intensity. The absence of dissolved CO during the period of growth of the Pt—CO band makes it clear that the reaction of dissolved CO with the platinum surface is rapid despite the fact that the platinum particles are dispersed in a polymer solution. The fact that an increase in dissolved CO concentration by at least a factor of ten between 1 and 15 min results in no further increase in intensity of adsorbed CO implies also that the equilibrium between free (dissolved) CO and adsorbed CO strongly favours the adsorbed state.

The measured coverage dependent frequency shift in the IR absorption for linearly adsorbed CO on **Pt-15** is 25 cm^{-1}. However, the lowest absorbance measured on the colloidal particles is already 13% of that corresponding to maximum coverage. We can therefore assume that the full frequency shift in going from the lowest coverage to saturation will be greater than the 25 cm^{-1} that we observe. As described above, shifts of this magnitude are indicative of the presence of absorptions corresponding to two (or more) coupled vibrational modes in the spectrum, implying the presence of a hidden absorbance at even lower frequency than 2040 cm^{-1}. The fact that there is no sign of separate absorptions in the saturation ^{12}CO spectrum of **Pt-15** may be a reflection of the resolution of our experiment, or of the fact that in vibrationally coupled systems a low frequency component may be invisible even when it comprises 90% of the adlayer, due to intensity transfer to the higher frequency band.[40,44]

Assuming that this shift has an origin similar to the shifts observed on crystalline platinum surfaces, that is the vibrational coupling between CO oscillators adsorbed in domains on the surface of the platinum particles, this means that at a particle diameter of 1.5 nm, which corresponds to 5–6 atomic diameters, the surface of the particle offers arrays of adsorption sites of sufficient extent and regularity to allow vibrational coupling to be observed between CO molecules in the adsorbed overlayer. In the absence of bands due to CO on terrace sites, this must involve coupling between one-dimensional arrays of CO on edges and on other defect sites.

$^{12}CO/^{13}CO$ exchange spectra. In isotopic exchange experiments on **Pt-10** and **Pt-15**, exchange was sufficiently rapid in both cases to allow complete replacement of one isotopomer by the other within approximately one hour, as shown in Fig. 5(*a*) and 5(*b*). We note that the intensities of the bands corresponding to maximum ^{13}CO coverage are, in all of the cases reported here, less than the corresponding intensities for the maximum ^{12}CO coverage samples. This could imply that the initial ^{13}CO coverage might not have been maximal. However, since initial saturation of the colloidal metal with ^{13}CO was checked by passing ^{13}CO through the colloidal suspension until constant intensity was observed this seems unlikely, and the origin of the discrepancy probably lies in the dependence of the extinction coefficient on the relative reduced masses of ^{12}CO and ^{13}CO (as pointed out by a referee).

At 100% ^{13}CO, IR absorbances for linear CO are observed at 1999 and 1998 cm^{-1} for **Pt-10** and **Pt-15**, respectively. During addition of ^{12}CO these absorptions decrease as a higher frequency band increases in intensity over the course of the exchange reaction, and at 100% ^{12}CO the corresponding frequency in both cases is 2045 cm^{-1}. There is an immediately obvious difference between **Pt-10** and **Pt-15** spectra. In the case of **Pt-10** both absorptions remain at constant frequency as ^{12}CO replaces ^{13}CO, and an isosbestic point (a fixed frequency of constant absorbance) is observed between the two. However, in the case of **Pt-15** the high frequency component of the linear CO absorption increases in frequency as the concentration of ^{12}CO on the surface increases, while the lower frequency component shows little change, and no isosbestic point results.

We propose that the presence or absence of the isosbestic point is diagnostic of the absence or presence of vibrational coupling between adsorbed CO molecules, based on the following considerations. In order for a point of constant absorbance to be observed in the spectra of a system in which two chromophores *a* and *b* are interconverting, certain criteria must apply.[45] The spectra of **a** and **b** must, of course, intersect, and the sum of the concentrations [**a**] + [**b**] must be constant. These conditions are clearly met for an exchange of ^{13}CO with ^{12}CO in a closed system of fixed surface area and so apply to both the 1.0 and 1.5 nm Pt sols. However, these preconditions also assume that the extinction coefficients ε_a and ε_b of the two species at each wavelength remain the same during the interconversion, which means that the band profiles must be independent of concentration. When these conditions are met there will be one or more points in the superimposed spectra of the interconverting species **a** and **b** at which the condition ε_a[**a**] + ε_b[**b**] = constant, and this wavelength defines an isosbestic point, a point of constant absorbance. In the cases under discussion here, an isosbestic point for the isotopically exchanging CO overlayer would be expected only if adsorbed CO molecules vibrate independently, with no coupling, giving spectra corresponding to an ideal interconverting system (assuming that the extinction coefficients for the bands were coverage independent).

In small particulate systems, it is to be expected that vibrational coupling might be removed if the particle is too small to posess faces of sufficient size to assemble the requisite domains of CO. This might also arise for larger particles if their surfaces have a high incidence of defects. In such a system fre-

quency shifts and intensity transfer would be greatly reduced, thus approximating the conditions for an isosbestic point. On this basis, the conclusion we draw from the occurrence of the isosbestic point in Fig. 6(*a*) is that the surface of the **Pt-10** sol does not permit the assembly of domains of vibrationally coupled CO molecules, probably by virtue of the small size of the particles. However, when the vibrational spectra of adsorbed ^{13}CO–^{12}CO mixtures on metal surfaces display non-linear effects (coverage dependent frequency and intensity transfer) due to vibrational coupling, one or more of the pre-conditions for an isosbestic will be destroyed during ^{13}CO–^{12}CO exchange. As described above and shown in Fig. 2, the shift in frequency with coverage for ^{12}CO on **Pt-15** shows the operation of vibrational coupling, and we may therefore assume that intensity transfer is also occurring in the spectra in Fig. 6(*b*). Thus, the conditions for an isosbestic point are removed, with the result shown.

These exchange spectra simply confirm the presence of coupling for CO on **Pt-15** observed in the partial coverage experiment. However, for **Pt-10** it is possible to conclude the absence of coupling from full ($^{13}CO + {}^{12}CO$) coverage experiments without the possibly disruptive consequences of decarbonylation of the as-prepared CO-covered sample by maintaining a CO saturated surface of changing isotopic composition throughout the exchange experiment.

Conclusions

The experiments described demonstrate that the adsorption of CO on colloidal metals in liquid dispersion can be quite easily investigated by infrared spectroscopy. In addition to the assignment of absorption bands at maximum coverage, partial coverage spectra and isotopic exchange experiments, which can be routinely performed, reveal details of the surface structure of the metal particles. The results obtained for two Pt–PVP colloids indicate that the surfaces of such materials contain a high incidence of defect sites and that smooth terraces are not detectable. In light of recent high resolution microscopy on apparently regular monocrystalline Pt colloids, we conclude that such surface irregularity is probably to be found for colloidal metal particles in most, if not all, cases where the preparation conditions do not lead to annealing of the as-prepared surface.

Acknowledgements

The authors acknowledge helpful discussions with Dr. D. Blackmond (M.P.I.). A post-doctoral fellowship from the Max-Planck-Gesellschaft to D. de C. is gratefully acknowledged.

References

1 J. S. Bradley, J. M. Millar, E. W. Hill and M. Melchior, *J. Chem. Soc., Chem. Commun.*, 1990, 705.
2 J. S. Bradley, J. M. Millar, E. W. Hill and S. Behal, *J. Catal.*, 1991, **129**, 530.
3 J. S. Bradley, J. M. Millar, E. W. Hill, S. Behal, B. Chaudret and A. Duteil, *Faraday Discuss. Chem. Soc.*, 1991, **92**, 255.
4 J. S. Bradley, E. W. Hill, S. Behal, C. Klein, B. Chaudret and A. Duteil, *Chem. Mater.*, 1992, **4**, 1234.
5 A. Duteil, R. Quéau, B. Chaudret, R. Mazel, C. Roucau and J. S. Bradley, *Chem. Mater.*, 1993, **5**, 341.
6 J. S. Bradley, E. W. Hill, B. Chaudret and A. Duteil, *Langmuir*, 1995, **11**, 693.
7 J. S. Bradley, E. W. Hill, C. Klein, B. Chaudret and A. Duteil, *Chem. Mater.*, 1993, **5**, 254.
8 J. S. Bradley, G. H. Via, L. Bonneviot and E. W. Hill, *Chem. Mater.*, 1996, **8**, 1895.
9 D. de Caro and J. S. Bradley, *Langmuir*, 1997, **13**, 3067.
10 D. de Caro and J. S. Bradley, *Langmuir*, 1998, **14**, 245.
11 L. N. Lewis and N. Lewis, *J. Am. Chem. Soc.*, 1986, **108**, 7228.
12 M. R. Mucalo and R. P. Cooney, *J. Colloid Interface Sci.*, 1992, **150**, 486.
13 M. R. Mucalo and R. P. Cooney, *J. Chem. Soc., Faraday Trans.*, 1991, **87**, 1221.
14 M. R. Mucalo and R. P. Cooney, *Can. J. Chem.*, 1991, **69**, 1649.
15 M. R. Mucalo and R. P. Cooney, *J. Chem. Soc., Chem. Commun.*, 1989, 94.
16 M. R. Mucalo and R. P. Cooney, *Chem. Mater.*, 1991, **3**, 1081.
17 R. K. Brandt, M. R. Hughes, L. P. Bourget, K. Truszkowska and R. G. Greenler, *Surf. Sci.*, 1993, **286**, 15.
18 M. R. Mucalo and R. P. Cooney, *J. Chem. Soc., Faraday Trans.*, 1991, **87**, 3779.
19 R. Van Hardeveld and F. Hartog, *Adv. Catal.*, 1972, **22**, 75.
20 L.-L. Sheu, Z. Karpinski and W. M. H. Sachtler, *J. Phys. Chem.*, 1989, **93**, 4890.
21 N. Sheppard and T. T. Nguyen, in *Advances in Infrared and Raman Spectroscopy*, ed. R. J. Clarke and R. E. Hester, Heyden and Son, London, 1978, p. 106.
22 A. Rodriguez, C. Amiens, B. Chaudret, M.-J. Casanove, P. Lecante and J. S. Bradley, *Chem. Mater.*, 1996, **8**, 1978.
23 K. Moseley and P. Maitlis, *J. Chem. Soc., Chem. Commun.*, 1971, 982.
24 R. G. Greenler, K. D. Burch, K. Kretzschmar, B. Klauser, A. M. Bradshaw and B. E. Hayden, *Surf. Sci.*, 1985, **153/3**, 338.
25 P. S. Braterman, *Metal Carbonyl Spectra*, Academic Press, London, 1975.
26 D. G. Duff, P. P. Edwards and B. F. G. Johnson, *J. Phys. Chem.*, 1995, **99**, 15934.
27 J. Köhler and J. S. Bradley, *Catal. Lett.*, 1997, **45**, 203.
28 J. U. Köhler and J. S. Bradley, unpublished results.
29 Z. L. Wang, T. S. Ahmad and M. A. El-Sayeed, *Surf. Sci.*, 1997, **380**, 302.
30 T. S. Ahmadi, Z. L. Wang, T. C. Green, A. Henglein and M. A. El-Sayeed, *Science*, 1996, **272**, 1924.
31 T. S. Ahmadi, Z. L. Wang, A. Henglein and M. A. El-Sayeed, *Chem. Mater.*, 1996, **8**, 1161.
32 R. Van Hardeveld and F. Hartog, *Surf. Sci.*, 1969, **15**, 1889.
33 R. F. Willis, A. A. Lucas and G. D. Mahan, in *The Chemical Physics of Solid Surfaces and Heterogeneous Catalysts*, ed. D. A. King and R. P. Woodruff, Elsevier, Amsterdam, 1983, vol. 2, pp. 59.
34 P. Hollins and J. Pritchard, *Prog. Surf. Sci.*, 1985, **19**, 275.
35 R. P. Eischens and W. P. Pliskin, *Adv. Catal.*, 1958, **10**, 1.
36 A. Crossley and D. A. King, *Surf. Sci.*, 1977, **68**, 528.
37 P. Hollins and J. Pritchard, *Chem. Phys. Lett.*, 1980, **75**, 378.
38 B. E. Hayden, K. Kretzschmar, A. M. Bradshaw and R. G. Greenler, *Surf. Sci.*, 1985, **149**, 395.
39 R. G. Greenler, F. M. Leibsle and R. S. Sorbello, *Phys. Rev. B*, 1985, **32**, 8431.
40 S. G. Fox, V. M. Browne and P. Hollins, *J. Electr. Spectrosc. Related Phenom.*, 1990, **54/5**, 749.
41 M. Moskovits and J. E. Hulse, *Surf. Sci.*, 1978, **78**, 397.
42 P. Hollins, *Surf. Sci.*, 1981, **107**, 75.
43 B. N. J. Persson and R. Rydberg, *Phys. Rev. B.*, 1981, **24**, 6954.
44 P. Hollins, *Spectrochim. Acta, Part A*, 1987, **43**, 1539.
45 M. D. Cohen and E. Fischer, *J. Chem. Soc.*, 1962, 3044.

Received in Montpellier, France, 25th May 1998;
Paper 8/03934H